DALTON
FULL PAPER

Magnetic structure and covalence in tetrachlorobis(*N*-phenylacetamidinato)rhenium(IV) by neutron diffraction

Philip A. Reynolds,[*a] **Brian N. Figgis**[b] **and David Martín y Marero**[c]

[a] *Research School of Chemistry, Australian National University, Canberra, ACT 0200, Australia*
[b] *Department of Chemistry, University of Western Australia, Nedlands, WA 6009, Australia*
[c] *ISIS Facility, Rutherford-Appleton Laboratory, Chilton, Didcot, Oxfordshire, UK OX11 0QZ*

Received 11th January 1999, Accepted 26th January 1999

Powder neutron diffraction measurements have been made at 2 and 20 K for the complex *cis*-[$ReCl_4$(NH=CMeNHPh)$_2$]. The changes in diffracted intensities on magnetic ordering at 9.7(1) K were fitted in the Shubnikov group $Pc'c'n$ to an antiferromagnetically ordered magnetic structure in which the spins are aligned along *c* in this orthorhombic crystal. A moment of 2.58(6) μ_B resides on the rhenium site in each molecule, while each chlorine site has a spin population of 1.03(8) μ_B due to covalent spin delocalisation. The N–C–N region of the other two ligands each has a spin population of $-1.86(10)$ μ_B, indicating a substantial spin polarisation resulting from electron correlation effects. The antiferromagnetic structure is consistent with a reinterpretation of earlier single crystal magnetisation data. The very large amounts of spin transfer observed within the molecule are not unexpected in this heavy metal complex, and qualitatively reasonable given a synergistic interaction between the two ligand types. The previous observation of a metamagnetic transition in this crystal is explained as being driven by a change in canting angles within the molecule, from alignment closely along *c* to an arrangement in which opposite halves of the molecule are differently canted, with small but significant $+b$ and $-b$ components. The direction of magnetisation within the molecule is thus not all parallel.

Studies of metal–ligand bonding by examination of magnetisation densities in transition metal complexes can provide unique information about covalence, spin polarisation and other effects in the molecular ground state. In this paper we study by powder neutron diffraction the complex *cis*-[$ReCl_4$(NH=CMeNHPh)$_2$], Fig. 1, in which the combination of a heavy metal and polarisable ligands produces major bonding effects on the magnetisation density. In addition, further light is thrown on the unusual metamagnetic magnetic ordering effects in this compound which were previously observed by SQUID magnetisation measurements at low temperatures.[1]

Covalent bonding in transition metal complexes can be studied both by polarised neutron diffraction (PND) to measure the magnetisation density in single crystals in an applied magnetic field, and by X-ray diffraction to measure the charge density. An example is the series of measurements on the hexaaquametal(II) ions in the Tutton salt series [ND_4]$_2$[M^{II}(D_2O)$_6$][SO_4]$_2$, M = V to Cu, where the different effects of σ and π covalent bonding, metal configuration, spin polarisation and spin–orbit coupling may be unravelled.[2–11] Studies on heavy transition metal complexes, where such effects are expected to be even larger, began with the study of caesium molybdenum(III) alum,[12] and has continued with [$AsPh_4$][$TcNCl_4$][13,14] and tris(acetylacetonato)ruthenium(III).[15]

The PND experiments require large single crystals and those are usually difficult to obtain in heavy metal complexes. However we have recently shown that neutron powder diffraction patterns of sufficient accuracy and stability can be obtained such that useful magnetic intensities can now be derived by subtraction of high intensity nuclear peaks which have been measured with and without an applied magnetic field.[16] In the compound [$Mn_{12}O_{12}(CD_3CO_2)_{16}(D_2O)_4$]·$2CD_3CO_2D$·$4D_2O$ it was possible to identify within the $S = 10$ ground state the relative orientations and sizes of spins on the manganese sites, and also gain some information on covalence.

We now apply this technique to the compound [$ReCl_4$(NH=CMeNHPh)$_2$], with the slight difference that to obtain the magnetic intensities here we subtract the powder neutron diffraction intensities at temperatures above a magnetic ordering transition and below it. This technique differs from the usual schemes in antiferromagnets, in that we are not searching only for new small peaks which appear due to magnetic

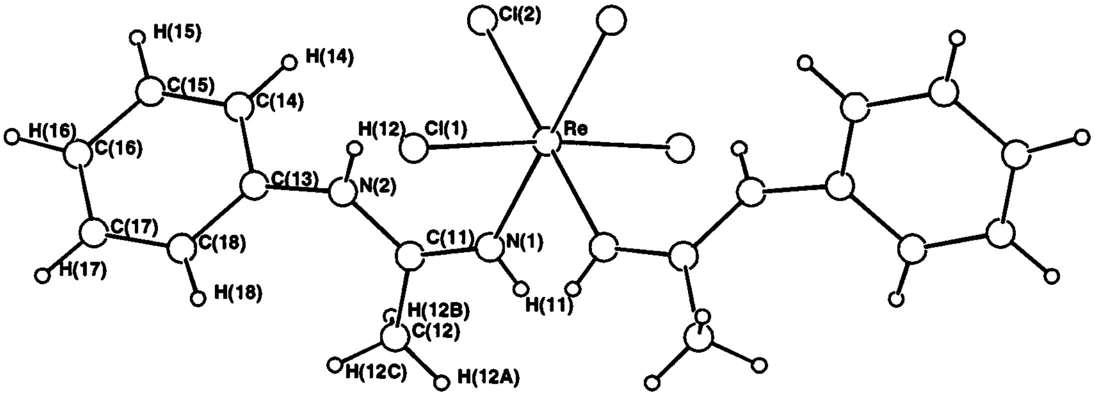

Fig. 1 The molecule *cis*-[$ReCl_4$(NH=CMeNHPh)$_2$]. A unique set of atoms are labelled.

scattering. Here, we are also relying on the subtraction process to reveal magnetic intensities augmenting already strongly allowed nuclear scattering peaks.

Compounds of formula $Re^{IV}Cl_4L_2$ (L = ligand)[17] are often of the high-spin category, which is unusual for heavy metal compounds. The high-spin feature is a strong advantage for accuracy in both the PND experiment and powder magnetic experiments. Spin transfers involving halogen ligands are often substantial, as evidenced by the PND studies on Cs_3CoCl_5[18] and $[AsPh_4][TcNCl_4]$.[13,14] Extensively π-delocalised ligands also show large effects, as in cobalt(II) phthalocyanine[19] and *cis*-$[Fe(bipy)_2Cl_2][FeCl_4]$.[20] Furthermore $[ReCl_4(NH{=}CMeNHPh)_2]$ can be grown to large crystal sizes.[1,21,22] It is thus a promising candidate for a full PND study to amplify our previous partial study with the magnetic field along the *b* axis.[1]

SQUID Magnetisation measurements have indicated that at low temperatures this material is probably a metamagnet.[1] Metamagnets are systems in which competing interactions are such that, at temperatures below a Neel point, the application of a modest magnetic field causes a sudden transition from an antiferromagnetic phase to one with a ferromagnetic component, often an aligned paramagnet.[23] Examples are $[Me_3NH][CoCl_3]\cdot 2H_2O$,[24] $CsCoCl_3\cdot 2D_2O$[25] and the more complex materials $[Fe(C_5Me_5)_2][TCNQ]$[26] (TCNQ = tetracyanoquinodimethanide) and a manganese Schiff base–ferricyanide complex.[27] Such magnetic alignment, depending on its type, often precludes useful PND experiments, but the present complex may be an exception. Our previous PND study examined the small ferromagnetic component in the metamagnet, and thus is not simply related to the molecular spin density. We therefore undertook this unpolarised powder diffraction study to examine the nature of the ordered magnetic phase, both because metamagnetism is itself uncommon and also to see if PND could be performed profitably by correct choice of conditions. An added attraction is that we may also gain some information about the molecular spin distribution.

Experimental and results

Neutron diffraction

A fine powder of $[ReCl_4(NH{=}CMeNHPh)_2]$ (1.8 g), prepared as before,[1,21] was placed in a cadmium shielded aluminium cell suitable for back reflection. It was mounted in a 100 mm bore liquid helium cryostat with sample heater and Rh/Fe resistance thermometer on the IRIS device at the ISIS spallation neutron source at the Rutherford-Appleton Laboratory. Time-of-flight neutron diffraction patterns were obtained over 2 d at temperatures of 20(1) and 2(1) K. The diffraction detector of the IRIS spectrometer is situated in near backscattering geometry. This configuration provides high resolution of up to $\Delta d/d \approx 2.5 \times 10^{-3}$ almost constant over the measured range. The 2 K pattern, assembled from several time-of-flight regions and corrected using vanadium scattering patterns in the standard way, is illustrated in Fig. 2 as a line joining the data points. The 20 K data are marked on this same graph as the crosses. It is instantly clear that the two datasets are almost identical.

Peak areas and positions were obtained from isolated peaks by Gaussian fitting. The small changes in intensity, *i.e.* the magnetic scattering, were obtained by subtraction of the areas. The instrumental resolution is such that even on temperature decrease from 20 to 2 K very small changes in peak positions due to altered cell dimensions are observed, and those cause direct subtraction to be inappropriate. No attempt was made to extract magnetic intensities where there was significant overlap of different unique peaks, except that in some cases where no magnetic intensity is observed then all peaks at that *d* spacing must have zero intensity, within the observed error σ. For *d* spacings of *ca.* 3.2 Å or less peak overlap became too severe to estimate magnetic intensities. Peaks treated for magnetic intensity are of two types, those allowed in the nuclear space group of *Pccn* and those forbidden. There were twelve of the former and sixteen of the latter containing, respectively, three and one reflection of intensity greater than 3σ. However, we note that the many "zeros" significantly constrain the relative spin populations, and are valuable observations.

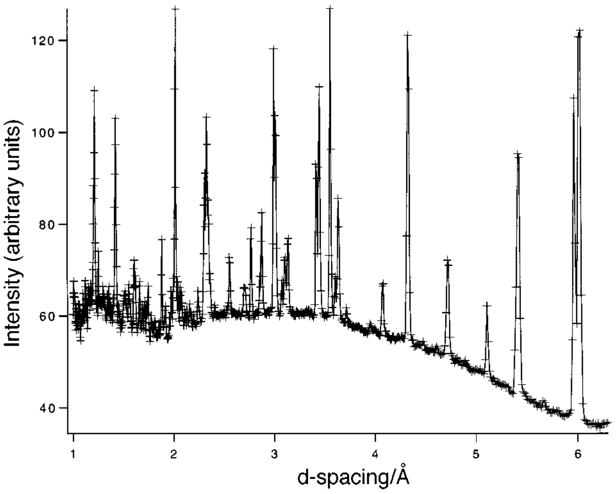

Fig. 2 The time-of-flight diffraction patterns from *cis*-$[ReCl_4(NH{=}CMeNHPh)_2]$ at 2 and 20 K measured on IRIS. The 2 K data are joined by the line, the 20 K data are the crosses.

The peak area intensity changes were converted into the square of the magnetic structure factor, $|F_M|^2$, by use of a model calculation of the neutron structure factors. The latter were estimated by use of the X-ray diffraction structure obtained at 92 K.[22] The parameters from this structure were adjusted in three ways, apart from the obvious change to use of neutron scattering lengths, to obtain a best estimate of the structure factors at 2 K. The cell size was changed to that observed, and nuclear positional coordinates were scaled in step to maintain a constant molecular geometry. The C–H and N–H bonds were lengthened to 1.08 and 1.01 Å respectively to compensate for the well known difference in hydrogen positions observed by X-ray and neutron scattering due to bonding effects. Lastly the thermal parameters were reduced to values appropriate for zero-point motion estimated from structures of similar materials observed at these low temperatures.[14,15,20] The resulting structure factors gave a consistent scale factor, with an error of *ca.* 5%, when compared to peak areas from the 2 K pattern. Such an error is insignificant when compared to that in the observed magnetic intensities. This scale factor was used to convert the observed magnetic intensities into $|F_M|^2$. A standard Rietveld fitting of the 2 K pattern is not possible given the number of variables which would be required. Subsequently determined single crystal structures by neutron[28] and X-ray diffraction[29] at 20 and 10 K respectively agree well with the structure as estimated above.

The subtraction process to obtain magnetic intensities relies on the assumption that the nuclear intensities at 2 and 20 K are not significantly different. At higher temperatures such an assumption would be unwarranted, mainly because of the roughly linear temperature dependence of the displacement parameters. For example an 18 K temperature change around 92 K would cause an increase of *ca.* 35 pm^2 in the typical displacement parameter,[22] causing a decrease in intensity at the shortest *d* spacing used in the magnetic subtraction of *ca.* 0.6%. Thus nuclear and magnetic intensity changes would be almost comparable. However at 20 K and lower we are in the regime where the displacement parameters are almost constant at the zero-point motion values. For example the average change in displacement observed between 10 and 20 K by X-ray and neutron diffraction is −2(2) pm^2.[28,29] The change in unit cell lengths between 2 and 20 K that we observe here is 8% of the

Table 1 Unit cell dimensions/Å at various temperatures. The 2 K cell is quoted, others are increments

	T/K						
Parameter	2	2–20	2–23	23, 0–7 T	23–26	2–92	2–293
a	21.608(8)	0.0044(5)	0.008(1)	0.0019(5)	0.0021(5)	0.069(4)	0.223(5)
b	7.262(2)	0.0000(5)	0.005(1)	0.0016(5)	0.0004(5)	−0.009(1)	0.138(2)
c	12.434(4)	0.0036(5)	0.005(1)	0.0029(5)	0.0029(5)	0.036(2)	0.091(3)

Table 2 Observed and calculated magnetic structure factor moduli squared (μ_B^2) at 2 K, arranged in order of d spacing

Reflection	$\|F_M(\text{obs.})\|^2$	$\|F_M(\text{calc.})\|^2$	Reflection	$\|F_M(\text{obs.})\|^2$	$\|F_M(\text{calc.})\|^2$
0 0 2	3(20)	0	2 1 0	0(20)	0
1 1 1	84(10)	88	4 0 1	44(20)	63
1 0 2	21(10)	0	4 1 0	0(20)	0
3 1 0	76(10)	85	5 0 0	0(20)	0
1 1 2	2(10)	2	0 0 3	0(20)	0
2 1 2	64(10)	74	5 0 1	0(20)	3
4 0 2	0(20)	0	1 0 3	0(20)	3
3 1 2	0(10)	11	2 0 3	0(20)	4
5 1 0	9(10)	6	0 1 3	0(20)	15
6 0 0	0(15)	0	3 0 3	0(20)	7
2 1 3	0(15)	11	1 2 0	0(20)	0
5 1 2	0(30)	13	4 0 3	0(20)	0
0 1 1	0(20)	1	3 2 0	0(20)	0
3 0 1	0(20)	3	6 1 0	0(20)	0

change between 2 and 92 K, that is the rate of change in cell length between 2 and 20 K is only 1/3 of the rate between 20 and 92 K. This is a further indication of the absence at low temperature of significant motion other than zero-point. An upper limit for the change in displacement between 2 and 20 K of 10 pm^2 produces a change in nuclear intensity of 0.2% for the most affected reflection that we use, and this is not significant.

In a previous run diffraction patterns were obtained in a cryomagnet at 23(2) and 26(2) K at zero applied field, and at 23(2) K in an applied magnetic field of 7 T. At these temperatures and fields magnetic scattering is not observed (see below) but we did observe both positive and negative peak intensity changes of a percent or two. These can be rationalised as realignment of magnetically anisotropic crystallites due to torque from the applied magnetic field. The net result, in this case, is to favour intensities from those reflections with Q, the momentum transfer, parallel to morphologically prominent crystal planes. This phenomenon does not occur in the 2 and 20 K data since no field was applied. In the previous case[16] it was avoided by cycling the magnetic field to mechanically settle the crystallites.

A collection of unit cell data is given in Table 1. This was obtained by least squares fitting of the same 18 peaks for each case. We have mainly quoted changes in cell parameters, since these are often more precise than the absolute values. The magnetic structure factor square moduli are given in Table 2. We notice that the estimated errors do not decrease below 10 μ_B^2. This may be compared to the strongest nuclear intensity of 5400 μ_B^2; a typical value for the reflections we have used is about one quarter of this. Thus we estimate that our measurement of total intensities has an accuracy of about 1% and the magnetic intensities only reach to a maximum of 8% of a typical nuclear intensity; most are much less.

A general conclusion is that, in this type of IRIS experiment, for significantly incoherently scattering molecules such as this the magnetic signal will become undetectable at magnetisations of less than *ca.* 0.03 μ_B per non-hydrogen atom. This is the case for our 23 K data where the magnetisation per Re is significantly less than 1 μ_B, at any crystal orientation. This may be alternatively expressed as that the magnetic signal of an $S = 1/2$ system will disappear into the noise for a molecule with more than *ca.* 30 non-hydrogen atoms per magnetic ion. Thus for useful data on most chemically interesting molecules a system with $S > 1/2$ is required.

Least-squares modelling

We fitted the magnetic intensities using a modified version of the program ASRED.[30] Here the molecular form factor was calculated using only a monopole model, given that our experimental resolution was insufficient to define any anisotropy around atom sites.[13] The atomic form factors used were from Hartree–Fock calculations,[31] using the spherical components from 2p for the carbon and nitrogen sites, 3p for the Cl and 5d for the Re. Additionally, the populations on the two independent chlorine and the two nitrogen sites were constrained to be equal. We required zero spin population on the phenyl ring, which is almost orthogonal to the Re–N–C–N amidine fragment, so that interactions of π type would be blocked, while those of σ type would be rapidly attenuated by intervening atoms. The total molecular spin population was constrained to 3.00, and the g factor used to convert this into magnetisation was taken as 1.86 by use of the high temperature SQUID result. Thus the number of population variables was three.

The magnetisation density within any given molecule was assumed to be everywhere parallel, but both the orientation in space and the relative orientations of different molecules' magnetisations were allowed to vary by use of two angular variables in the least squares process. As we show below, the first approximation is not strictly true, and there is some small relative canting within the molecule. However, this is calculated to have only a negligible effect on this unpolarised diffraction experiment, although the previous PND is greatly affected. The *Pccn* $Z = 4$ nuclear crystal structure allows one ferromagnetic and three antiferromagnetic relative molecular magnetisations. A superlattice ordering situation was rejected since there was no evidence for this.

Three starting points for the refinements were taken as (a) rhenium population of 3.00 spins and all others zero, (b) all eleven refined sites of equal spin population of 3/11 spin and (c) 3/4 spin only on each of the nitrogen sites. The first is a reasonable first guess, but we include the others to demonstrate that we do indeed reach a global minimum. The starting points for magnetisation directions were taken as the three principal axes. For three of the four magnetic arrangements the R factor stayed near a poor value of unity for all three spin starting arrangements. For one of the antiferromagnetic arrangements,

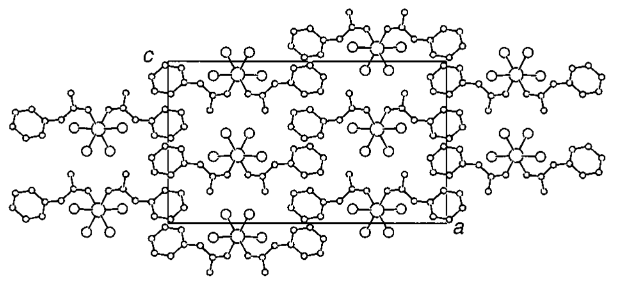

Fig. 3 The unit cell of *cis*-[$ReCl_4(NH{=}CMeNHPh)_2$], *ac* plane of projection.

the Shubnikov group *Pc′c′n* (no. 371),[32] the 5 parameter refinements, three spin arrangements and two magnetisation directions, all converged to the same structure with the easy axis of magnetisation refining to almost the *c* direction. The favoured *Pc′c′n* magnetic arrangement involves ferromagnetic interaction of molecules separated by [010], antiferromagnetic for those separated by [001/2], and antiferromagnetic between molecules at $\frac{1}{4},\frac{1}{4},z$ and $\frac{3}{4},\frac{3}{4},\frac{1}{2} - z$. The easy axis, by use of the SQUID data, was then fixed as *c*, and the three populations refined. The refinements reached $R(F^2) = 0.37$, with $R(F) = 0.12$ for reflections having $F^2 > 3\sigma(F^2)$; $\chi^2 = 0.43$. The final populations were: Re, 2.58(6); Cl, 1.03(8); N, −0.75(6); C, −0.36(13) spin. We note that we obtain four populations from three least squares variables since the total population [2.58 + 4 × 1.03 + 2(−0.36) + 2(−0.75)] is constrained to three spins. The experimental resolution is such that the spin populations of the N–C–N links on the acetamidino ligand are highly correlated, but localisation on one nitrogen rather than the other is not favoured. The structure factors calculated are listed in Table 2. We should emphasise again that the reflections of zero measured intensity play a strong role in the fitting. For example if we remove all four reflections of greater than 3σ significance and refine the model fixing only the rhenium population then we still obtain a chlorine population of +0.8 and NCN of −1.2 spins. The relative signs and sizes of the populations are partly determined by the zeros in magnetic intensity.

Discussion

Structure

The structure is discussed in more detail elsewhere,[22] and here we present only a summary of relevant details. The [$ReCl_4(NH{=}CMeNHPh)_2$] molecular packing in the unit cell is illustrated in Fig. 3. The molecules are extended along *a*, with interleaving phenyl groups. This extension facilitates separation of the hydrophobic phenylamidino and hydrophilic $ReCl_4$ units. The structure can be described as sheets of $ReCl_4$ units in the *bc* plane separated by layers of phenyl rings, which are themselves twisted at 68° to the Re–N–C–N plane. The Re···Re separations are 7.25 and 6.25 Å along *b* and *c* respectively, but the much longer distance of 11.6 Å along *a*. The Re atom is approximately *cis*-octahedrally co-ordinated by four Cl and two N atoms. This co-ordination produces a high spin $J = 3/2$ ground state, unusual in the heavy transition metals, while the large Re···Re separations result in weak magnetic exchange particularly along *a*.

The unit cell data are as expected. At higher temperatures the axes expand a little anisotropically. At lower temperatures, as the zero-point motion regime is entered, the coefficient of expansion drops markedly; indeed along *b* it becomes close to zero. Application of a 7 T magnetic field causes the cell volume at 23 K to increase, relatively isotropically, by 0.054(7)%, due to magnetoelastic coupling.

Magnetic ordering at zero applied magnetic field

The neutron diffraction experiment clearly indicates that the magnetic structure has the magnetic moments aligned along *c*, and has the orthorhombic magnetic space group *Pc′c′n*. This is an antiferromagnetic arrangement including, as an aid to visualisation, spin directions of +*c* on the rheniums at $\pm(\frac{1}{4},\frac{1}{4},z)$ and −*c* for those at $\pm(\frac{1}{4},\frac{1}{4},\frac{1}{2} + z)$.

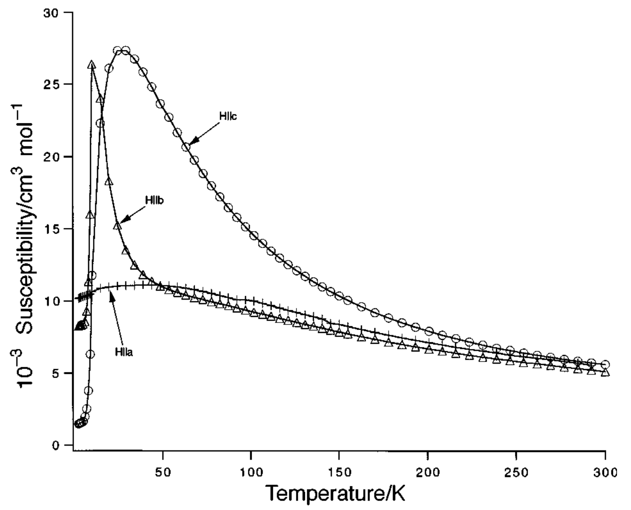

Fig. 4 The principal magnetic susceptibilities *versus* temperature using a magnetic field of 1.0 T.

The arrangement just mentioned is not compatible with the published single crystal susceptibility measurements.[1] Fig. 4 shows a reinterpretation of the susceptibility data of ref. 1 in which the data originally assigned to magnetic fields parallel to *a* and *c* have been swapped. This exchange of assignment, as shown in Fig. 4, renders the susceptibility and diffraction data compatible. The reason for this error in ref. 1 is an error in assigning those crystal faces which were then used to find the principal axes.[1] The unusual morphology consists of {413}, {110} and {100} faces, is quite variable, and the faces are often not very planar. Subsequent study of morphology by optical goniometry of very slowly grown crystals has corrected the initial incorrect assignment. The conclusions of ref. 1 are not greatly affected by this correction. The only major change is that the magnetic easy axis is now *c* rather than *a*. The high temperature SQUID data now indicate an Ising ordering arrangement with a zero-field splitting of −20(2) cm^{-1} and principal axis *c*. At lower temperatures the rise in the *b* susceptibility indicates a ferromagnetic interaction along *b*, which at even lower temperatures collapses, as do the other two principal susceptibilities, to give an antiferromagnetic ordered state with moments aligned along *c*. This state has now been confirmed by the neutron diffraction data, and of the three antiferromagnetic alternatives *Pc′c′n* is that observed.

The other interesting feature in the magnetic ordering is the metamagnetic behaviour. A phase transition is induced if a high field is applied along *b*, but not for *a* or *c*. We previously mapped this transition as a function of applied magnetic field and temperature, and located a tricritical point. The sudden increase in moment along *b* at high fields can now be assigned as a phase transition from the orthorhombic *Pc′c′n* structure to a highly canted ferrimagnetic monoclinic structure. The nature of the change in direction of the magnetic moment will be discussed after we have dealt with the molecular magnetic properties, since an explanation relies on an understanding of those latter quantities.

The *Pc′c′n* structure is one of the class of antiferromagnetic structures in which a PND experiment can give useful flipping ratios in zero applied magnetic field, in a similar way to ferromagnets. The conditions for this to be so are that there are no opposite spins on sites related by nuclear inversion or on those related by lattice translation,[33] and that is the case for *Pc′c′n*. Then there are two types of magnetic domains and they are related by a change of handedness. In order to obtain a non-zero flipping ratio the domain populations must be unbalanced. Since, unlike ferromagnets, for antiferromagnets a multidomain situation is of higher energy than single domain, this can sometimes occur spontaneously on cooling. However crystal defects can interfere with this process, requiring application of a driving force.

Our previous PND measurements with an applied field parallel to *b* measured only *l*-even reflections in the *ac* plane. These are affected only by the small ferromagnetic *b* axis magnetisation component, whose molecular distribution will be discussed below. Any possible magnetic scattering from *c* axis magnetisation would not have been seen, since for *l*-even *h*0*l* reflections the *Pc*′*c*′*n* magnetic structure gives magnetic structure factors of zero.

The molecular wavefunction

We shall now discuss covalence and the zero-field splitting in the light of our present diffraction results.

(a) Covalence and spin polarisation. We observe a great deal of spin transfer in this molecule; it is clearly very far from an ionic rhenium(IV) compound. Each chlorine has 1.03(8) spins, while each acetamidino ligand has −1.86(10) spins. The residue of 2.58(6) spins is located on the rhenium atom. The chlorine spin is clearly dominated by covalent effects, but that of the acetamidino ligand by spin polarisation. There is also probably substantial synergy between the covalence and the spin polarisation phenomena.

We can compare the chlorine spin population to previous PND and ESR results. In the $IrCl_6^{2-}$ ion ($S = 1/2$) various indirect estimates from the ESR results place from 40 to 84% of the single total spin on the chloride ligands.[34,35] This amount of covalence is at least twice that found by ESR for analogous first row transition metal complexes. Such increased covalence in heavier metal complexes is expected.[35] In our PND experiments on the $TcNCl_4^-$ ion ($S = 1/2$) we found 29(2)% of the single spin delocalised onto the four chlorine ligands. In the first row transition metal ions $CoCl_4^{2-}$ ($S = 3/2$) and $FeCl_4^-$ ($S = 5/2$) PND experiments show, respectively, only 10 and 17% of the spin on the four ligand chloride atoms.[18,20] We thus see a substantial increase in spin delocalisation on moving from first to the second to third transition metal series, as previously indirectly observed by ESR. In this particular case we are seeing an apparent 137% of the total spin on the chlorine atoms, about twice what we might have predicted from the above results. We believe this is due to the influence of the spin polarisation of the acetamidino ligands.

The acetamidino ligand population of −1.86(10) spins, located on nitrogens directly bonded to and at the third atom from the metal, is again in accord with previous observations of bonding in those metals where the spins are located in the d_π orbitals. In the $TcNCl_4^-$ ion the nitrogen population is −15(1)% of the spin,[13,14] while in cobalt phthalocyanine [Co(Pc)] the $S = 1/2$ ground state has −0.54 spins on the phthalocyanine ring and 1.54 on the cobalt atom.[19,36] The rhenium–acetamidino linkage most closely resembles the latter, so given the $S = 3/2$ ground state compared to $S = 1/2$ in [Co(Pc)], the very large negative population observed on the acetamidines, while suprising, is acceptable, particularly if there is synergy with the Re–Cl bonding.

We thus have a picture of the π bonding in which, because the Re is a third-row transition metal, there is a large amount of covalence. The Re–Cl bonding delocalises spin *from* the rhenium d_π orbitals onto the chlorines, while the acetamidino ligands spin-polarise orbitals, putting spin *onto* the Re, leaving negative spin behind on the ligands. These two processes interact, magnifying the net effect.

(b) Zero-field splitting. The susceptibility experiment shows that the zero-field splitting is large, $2D = -20(2)$ cm^{-1}, and oriented along the molecular two-fold axis, which is coincident with the crystal *c* axis.

In the axis system used there are σ bonding orbitals $5d_{z^2}$(A_1 symmetry in C_{2v}) and $5d_{xy}$ (B_2), and π bonding orbitals $5d_{x^2-y^2}$ (A_1), $5d_{xz}$ (B_2) and $5d_{yz}$ (A_2). Using the ligand field approximation, the relative ordering of the energies of the topmost A_1, A_2 and B_2 π orbitals containing the three unpaired spins, neglecting correlation, can be crudely estimated from the magnetic susceptibility measurements. The topmost orbital dictates the easy axis, and if the next orbital is close to it then the magnetic ordering of the system is less Ising-like and more *XY*-like in character. For example for energies $A_1 \ll A_2 = B_2$ we predict a magnetic *XY* system in the crystal *ac* plane. An energy ordering $A_1 \ll B_2 < A_2$ is what we might expect from the susceptibility measurements and the observed easy axis direction and this ordering should be reproduced by theoretical calculations.

Magnetic ordering and the molecular magnetic structure in an applied magnetic field

At any point in the molecule off the *z* axis at $x = 1/4$, $y = 1/4$ in the *Pc*′*c*′*n* structure with zero magnetic field the local magnetic moment can be arbitrarily aligned, but any moments in the *ab* plane at *x*,*y* must be *equal* to the direction and size of the moment at $\frac{1}{2} - x, \frac{1}{2} - y$. However, if the moment directions were governed by the symmetry of the nuclei, the *ab* moments at these two symmetry related positions would be *opposite* in sign, while the *c* moment would be the same. Since the moment direction is produced at least partly by the local molecular nuclear symmetry, this means that a net *c* moment is acceptable both on the grounds of nuclear symmetry and the observed *Pc*′*c*′*n* magnetic symmetry. However, any moments in the *ab* plane are disfavoured by these conflicting symmetry requirements. This does not mean that the *ab* moment is zero, however, since the requirement of *Pc*′*c*′*n* magnetic symmetry has been imposed by the experimental results. If the true magnetic symmetry were lower, but still close to *Pc*′*c*′*n*, then some *ab* moment becomes allowed.

Application of a field along *b* breaks the orthorhombic symmetry to give monoclinic, removing twofold symmetry, whether coloured or not, around the axis along *z* at $x = 1/4$, $y = 1/4$. Thus, for symmetry reasons we may expect some net *ab* moment to appear, of *opposite sign* for *x*,*y*,*z* and $\frac{1}{2} - x, \frac{1}{2} - y, z$, as a result of the molecular nuclear symmetry. This is of course in addition to the net moment induced along +*b* due to the applied field.

We assume the true zero-field magnetic symmetry is *Pc*′*c*′*n*. In this case, at zero field, this symmetry must be a result of the intermolecular exchange overpowering the intramolecular effect discussed above. Metamagnetic transitions involve the applied magnetic field tipping the balance between a local energy and a magnetic exchange energy whose influences are opposed. In this case this is mainly a rearrangement of *ab* magnetic moment such that the intermolecular exchange becomes less favourable and the intramolecular energy more favourable. The magnetic field encourages this since it causes the appearance of moment along *b*.

This discussion does result in an explanation of our previous PND results. Table 3 shows the observed moments along *b* on the left and right sides of the molecule. It also shows these quantities divided by the *c* moment which we have observed here. We previously pointed out that the net *b* moments in the first two columns could arise from a combination of variable canting, covalence and spin polarisation. Given the reasonable assumption that the magnetic field only cants pre-existing spin density, then the ratio of this *b* moment to the observed *c* moment gives the canting angles at various sites in the molecule. As we can see from Table 3, the rhenium site is canted

Table 3 Previous PND results. The first two columns are the *b* moments observed by PND, in $\mu_B \times 10^3$, for each side of the molecule. The last two columns are the ratio of these *b* moments to the *c* moments

Atom	Molecule left moment	Molecule right moment	Molecule left canting	Molecule right canting
Re	119(24)		0.046(9)	
Cl(1)	65(23)	−56(24)	0.063(23)	−0.054(25)
Cl(2)	118(30)	−21(18)	0.115(32)	−0.020(20)
N(1) + N(2)	−66(25)	68(35)	0.035(14)	−0.037(18)

+2.6(5)° towards *b*, the left side of the molecule +4(1)° towards *b*, and the right side −2(1)°, that is away from *b*. This arrangement is just as we expect, a net moment along *b*, but with a superimposed dipolar term in the canting direction giving opposing canting on either side of the molecule, so as better to match the molecular nuclear geometry.

Conclusion

Neutron powder diffraction has been used to obtain magnetic intensities by relying on the subtraction of patterns above and below a magnetic ordering transition to reveal magnetic intensities augmenting nuclear peaks. The methodology can be applied on high resolution long *d*-spacing diffractometers like IRIS or OSIRIS at ISIS, to systems with $S > 1/2$, since for $S = 1/2$ systems the magnetic signal disappears into the noise for most chemically significant molecules.

Of the possible magnetic structures, an orthorhombic magnetic space group $Pc'c'n$ with the magnetic moments aligned along *c* has been derived from the neutron diffraction experiment. This agrees with previous results from single crystal susceptibility measurements[1] after correction of an axis assignment error in the former paper. In this metamagnetic system a phase transition occurs after application of a magnetic field, changing from the orthorhombic to a highly canted ferrimagnetic monoclinic structure.

Substantial covalent delocalisation of spin is observed onto the chlorine sites. It is about twice the amount expected in this third transition series metal complex from extrapolation of results obtained in other first to third transition metal series complexes. Large amounts of negative spin are left on the acetamidine ligands when orbitals are spin polarised due to positive spin in the Re–Cl bonds. The concerted interaction of chloride and acetamidine ligands may be responsible for the substantial increase in spin delocalisation observed above that expected. This delicate and particular balance between the spins in the long quasi-one-dimensional π system of the bis(acetamidinato)rhenium fragment and those of the Re–Cl bonds may provide a severe test for theoretical calculation.

The magnetic structure is suitable for a full single crystal PND experiment if a crystal with unbalanced domain populations can be produced. This would provide much more detailed information and an attempt is worthwhile given the extreme covalence and polarisation effects revealed here.

Acknowledgements

We thank the Australian Research Council and Department of Industry, Trade and Tourism for financial support.

References

1 P. A. Reynolds, B. Moubaraki, K. S. Murray, J. W. Cable, L. M. Engelhardt and B. N. Figgis, *J. Chem. Soc., Dalton Trans.*, 1997, 263.
2 B. E. Fender, B. N. Figgis, J. B. Forsyth, P. A. Reynolds and E. J. Stevens, *Proc. R. Soc. London, Ser. A*, 1986, **404**, 127.
3 R. J. Deeth, B. N. Figgis, J. B. Forsyth, E. S. Kucharskii and P. A. Reynolds, *Proc. R. Soc. London, Ser. A*, 1989, **421**, 153.
4 B. N. Figgis,E. S. Kucharski, P. A. Reynolds and F. Tasset, *Proc. R. Soc. London, Ser. A*, 1990, **428**, 113.
5 C. D. Delfs, B. N. Figgis, J. B. Forsyth, E. S. Kucharski, P. A. Reynolds and M. Vrtis, *Proc. R. Soc. London, Ser. A*, 1992, **436**, 417.
6 B. N. Figgis, P. A. Reynolds and J. W. Cable, *Mol. Phys.*, 1993, **80**, 1377.
7 B. N. Figgis, E. S. Kucharski and P. A. Reynolds, *Acta Crystallogr., Sect. B*, 1990, **46**, 577.
8 B. N. Figgis, L. Khor, E. S. Kucharski and P. A. Reynolds, *Acta Crystallogr., Sect. B*, 1992, **48**, 144.
9 B. N. Figgis, C. J. Kepert, E. S. Kucharski and P. A. Reynolds, *Acta Crystallogr., Sect. B*, 1992, **48**, 753.
10 B. N. Figgis, B. B. Iversen, F. K. Larsen and P. A. Reynolds, *Acta Crystallogr., Sect. B*, 1993, **49**, 794.
11 B. N. Figgis, A. N. Sobolev, D. M. Young, A. J. Schultz and P. A. Reynolds, *J. Am. Chem. Soc.*, 1998, **120**, 8715.
12 S. P. Best, B. N. Figgis, J. B. Forsyth, P. A. Reynolds and P. L. W. Tregenna-Piggott, *Inorg. Chem.*, 1995, **34**, 4605.
13 B. N. Figgis, P. A. Reynolds and J. W. Cable, *J. Chem. Phys.*, 1993, **98**, 7743.
14 P. A. Reynolds, B. N. Figgis, J. B. Forsyth and F. Tasset, *J. Chem. Soc., Dalton Trans.*, 1997, 1447.
15 P. A. Reynolds, J. W. Cable, A. N. Sobolev and B. N. Figgis, *J. Chem. Soc., Dalton Trans.*, 1998, 559.
16 P. A. Reynolds, E. P. Gilbert and B. N. Figgis, *Inorg. Chem.*, 1996, **35**, 545.
17 *Comprehensive Coordination Chemistry*, eds. G. Wilkinson, R. D. Gillard and J. A. McCleverty, Pergamon, Oxford, 1987, vol. 4.
18 B. N. Figgis and P. A. Reynolds, *J. Phys. Chem.*, 1990, **94**, 2211.
19 P. A. Reynolds and B. N. Figgis, *Inorg. Chem.*, 1991, **30**, 2294.
20 B. N. Figgis, P. A. Reynolds and J. B. Forsyth, *J. Chem. Soc., Dalton Trans.*, 1988, 117.
21 G. Rouschias and G. Wilkinson, *J. Chem. Soc. A*, 1968, 489.
22 L. M. Engelhardt, A. N. Sobolev, P. A. Reynolds and B. N. Figgis, *Aust. J. Chem.*, 1996, **49**, 489.
23 E. Stryjewski and N. Giordano, *Adv. Phys.*, 1977, **26**, 487.
24 H. A. Groenendijk and A. J. van Duyneveldt, *Physica B*, 1982, **115**, 41.
25 A. L. M. Bongaarts and W. J. M. de Jonge, *Phys. Rev. B*, 1977, **15**, 3424.
26 J. S. Miller, J. H. Zhang, W. M. Rieff, D. A. Dixon, L. D. Preston, A. H. Reis, Jr., E. Gebert, M. Extine, J. Troup, A. J. Epstein and M. D. Ward, *J. Phys. Chem.*, 1987, **91**, 4344.
27 H. Miyasaka, N. Matsumoto, H. Okawa, N. Re, E. Gallo and C. Floriani, *Angew. Chem., Int. Ed. Engl.*, 1995, **34**, 1446.
28 P. A. Reynolds, R. Henning and A. J. Schultz, to be published
29 P. A. Reynolds, A. N. Sobolev and B. N. Figgis, to be published.
30 B. N. Figgis, P. A. Reynolds and G. A. Williams, *J. Chem. Soc., Dalton Trans.*, 1980, 2339.
31 E. Clementi and C. Roetti, *At. Data Nucl. Data Tables*, 1974, **14**, 177.
32 C. J. Bradley and A. P. Cracknell, *The mathematical theory of symmetry in solids*, Clarendon Press, Oxford, 1972.
33 H. A. Alperin, P. J. Brown, R. Nathans and S. J. Pickart, *Phys. Rev. Lett.*, 1962, **8**, 237.
34 J. H. E. Griffiths, J. Owen and I. M. Ward, *Proc. R. Soc. London, Ser. A*, 1953, **219**, 526.
35 J. H. M. Thornley, *J. Phys. C*, 1968, **1**, 1024.
36 G. A. Williams, B. N. Figgis and R. Mason, *J. Chem. Soc., Dalton Trans.*, 1981, 734.

Paper 9/00293F